Investigation of a novel bio-based phase change material hemp concrete for passive energy storage in buildings

Mohamed Sawadogo, Ferhat Benmahiddine, Ameur El Amine Hamami, Rafik Belarbi, Alexandre Godin, Marie Duquesne

Investigation of a novel bio-based phase change material hemp concrete for passive energy storage in buildings

Mohamed Sawadogo [1,3], Ferhat Benmahiddine [1], Ameur El Amine Hamami [1], Rafik Belarbi [1,*], Alexandre Godin [2] and Marie Duquesne [3]

[1] La Rochelle Université, LaSIE UMR CNRS 7356, Avenue Michel Crépeau, CEDEX 1, 17042 La Rochelle, France; mohamed.sawadogo@univ-lr.fr (M.S.); ferhat.benmahiddine1@univ-lr.fr (F.B.); ameur_el_amine.hamami@univ-lr.fr (A.H.); rafik.belarbi@univ-lr.fr (R.B.)
[2] Amplitude, 11 Avenue de Canteranne, Cité de la Photonique, Bâtiment MEROPA, 33600 Pessac, France; alexandre.godin@amplitude-laser.com (A.G.)
[3] Bordeaux INP, CNRS, Université de Bordeaux I2M, Bât A11, 351 Cours de la Libération, 33400 Talence, France ; marie.duquesne@u-bordeaux.fr (M.D.)

***** Correspondence: rafik.belarbi@univ-lr.fr

Featured Application: Passive latent heat storage for building applications, thermal comfort.

Abstract: In latent heat storage, energy is stored through the change of state of a material and then released when the material returns to its original phase. Latent heat thermal energy storage systems incorporate phase change materials (PCMs) as storage materials. The objective of this study is the fabrication and characterisation of a biosourced PCM hemp concrete. Hemp shives are vacuum impregnated with CA with an incorporation rate of 53%. The resulting shape-stabilized hemp shives/CA composite is used to fabricate PCM hemp concrete. The morphology and thermophysical properties of the materials at all stages (from pure CA to hemp concrete PCMs) are characterized using differential scanning calorimetry (DSC), scanning electron microscopy (SEM) and compared to the reference state (hemp concrete without PCMs). Results of the DSC measurement indicated melting and solidification temperatures hemp shives/CA composite of 28.9°C and 23°C, respectively and enthalpy of melting and solidification calculated as 78.7 and 76.4 $J.g^{-1}$, respectively. The TGA/dTG results indicated that the form stable composite exhibits good thermal stability under 170°C, making it suitable for building application. The thermal performances of PCM and reference hemp concrete are evaluated in a climatic chamber and compared to those of a reference hemp concrete. Results showed a good thermoregulation capacity of the PCM hemp concrete with a maximum time shift of 30 minutes and a temperature difference between reference and PCM hemp concrete of about 4.6°C.

Keywords: Bio-based shape-stabilized phase change material composite, latent heat thermal energy storage, hemp concrete, thermal performances.

1 Introduction

The building sector is the biggest energy consumer accounting for 40% in the total world energy consumption [1]. In the context of climate change [2], it is necessary to reduce the energy consumption at the worldwide level. The building sector is one of the key factor to achieve this goal. In order to reduce the energy consumption of buildings, essentially used for heating and cooling, it is important to decrease their energy consumption by better insulation or thermal

energy storage. The latter consists in capturing the thermal energy from internal heat gains or renewables, such as solar, at one time to use it later. The main advantages of thermal energy storage are: reduction of the energy consumption, limitation of heat losses, shift of electricity consumption from peak to off-peak periods and development of the use of intermittent renewable energy sources [3].

Numerous studies have shown that latent heat thermal energy storage (LHTES) which incorporates phase change materials (PCMs) is an efficient technique to increase the thermal capacity, energy efficiency and comfort impact of buildings [4–10]. The PCMs of interest in this work are solid-liquid ones. The basic principle of the LHTES based on liquid-solid transition is the following: during the melting process, the excess of thermal energy from the ambient is stored as latent heat in the PCMs and restored to the environment when the temperature drops below the temperature of solidification of the PCMs. In this study, the targeted application is the passive LHTES. In passive systems, the heat transfer fluid does not contribute to the storage and circulates naturally without any mechanical device. Silva et al. [11] studied the thermal performances of a south facing window shutter containing PCMs in a test cell located in Aveiro, Portugal, during summer. The results showed a thermal regulation capacity of the internal temperature of about 18–22% and temperature peaks delayed by 45 minutes to one hour compared to the reference compartment. Lee et al. [12] integrated paraffin with a melting temperature of 28–30°C into cellulose wall insulation. The incorporation of paraffin in the insulation reduced the heat flux from 16.1% to 38.5%. The maximum heat flow was delayed from 1.5 to 3 hours, which would allow reducing the electricity bill. Umberto et al. [13] investigated the thermal performances of two test cells, one as a reference and the other one containing a composite PCM system, comprised of two PCMs products with melting temperatures of 21.7°C and 25°C. The results indicated improved performances of the test cell containing the PCM composite system in lowering the maximum interior and surface temperatures by up to 6°C.

Many studies has been conducted in order to select the suitable PCM for a specific application. Jinghua et al. [14] investigated numerically the effects of the phase transition temperature, layer thickness and phase transition temperature radius of PCM on the performances of a roof with outer-layer shape-stabilized PCM. The optimal phase change temperature were 31–33 °C, 34–36 °C, 36–38 °C, 34–36 °C, and 29–31 °C respectively in severe cold region, cold region, hot summer and cold winter region, hot summer and warm winter region and mild region. Al-Rashed et al. [15] compared three PCM (RT-31, RT-35 and RT-42) with different melting temperatures in terms of reduction of the heat gains in the Kuwaiti hot climate region. The best results (energy saving as well as CO_2 saving) were obtained for RT-31, a PCM with phase change temperature of 27–33 °C compared to other PCM. Meng et al. [16] suggested a combined PCM with low (17-19°C) and high (28-30°C) melting temperatures allowing both energy storage in winter and summer.

These studies have shown the interest of incorporating PCMs in buildings envelopes. For this purpose, four different techniques have been used to integrate PCMs into building envelopes: direct incorporation, immersion, encapsulation and shape-stabilization [9,17–19]. A recent

literature review [20] allowed the identification of shape-stabilized PCMs as a promising technique to incorporate PCMs in buildings. Shape-stabilized PCMs are obtained by impregnating PCMs into porous building materials preventing leakage problems during the phase change process. This technique is simple, inexpensive, possesses a high impregnation rate compared to other techniques and is compatible with a wide variety of support materials. Biosourced materials, in particular, insulating materials such as hemp, flax and bamboo with their good porous structure are promising for the fabrication of shape-stabilized PCMs. This will allow the fabrication of a 100% bio-based PCMs composites.

The solid-liquid PCMs are classified in three groups: organics, inorganics and eutectic mixtures [21]. Organic PCMs are the most widely used for thermal energy storage due to their suitable melting/solidification temperature, high energy storage density, chemical stability and storage capacity [22]. Recently, fatty acids has gained of interest due to their suitable thermophysical properties such as high-energy capacity, congruent melting, solidification behaviour as well as good chemical and thermal stability [6,22–28]. Additionally, they have no toxicity, no corrosivity, small or no undercooling, small volume change during phase change and easy production from vegetable and animal oils [23].

Only few of these fatty acids possess a melting temperature in the range of the thermal comfort (15 to 30°C,T) [8,22]. However, the melting temperature of the PCMs can be adjusted to this climatic requirement by preparation of fatty acids eutectic mixtures. Duquesne et al. [25,29] have prepared two eutectics mixtures of capric and myristic acid, capric and palmitic acid with melting temperature of 24.29°C and 26.25°C. Ke et al. [30] have prepared a series of binary and multiple fatty acid eutectics by using five fatty acids (i.e. capric acid (CA), lauric acid (LA), myristic acid (MA), palmitic acid (PA), and stearic acid (SA), respectively). The melting temperature of the tested materials were found between 15-53°C.

The objective of this work is to fabricate a new composite PCM hemp concrete. Many researchers have identified hemp concrete as a good insulation material with promising physical and hygrothermal properties [31–34]. Coupled with the aforementioned PCMs excellent properties, the composite material is expected to possess excellent properties and suitable for LHTES application in building envelopes. The novelty of this study is the development of a bio-based PCM hemp concrete followed by a troughout properties characterization and thermal performances test of the developed materials. The PCM hemp concrete is intended to be used as an insulating element in building envelopes. For this purpose, hemp shives with a high porous structure are impregnated with CA, a pure fatty acid with melting temperature within the thermal comfort range. Vacuum impregnation method is used to fabricate shape-stabilized PCMs composites with improved thermal properties and without leakage. The novel 100% bio-based PCM composite is then used to fabricate PCM hemp concrete. The morphology and thermophysical properties of the materials at all stages (from pure CA to PCM hemp concrete) are characterized using differential scanning calorimetry (DSC), scanning electron microscopy (SEM) and compared to the reference state (hemp concrete without PCMs). Finally, the thermal

performances of the novel PCM hemp concrete are studied in a climatic chamber and compared to the reference hemp concrete.

2 Materials and methods

2.1 Materials

2.1.1 Selection of the PCM

The PCM must meet several selection criteria in order to be used effectively as a thermal energy storage material. Schröder and Gawron [35] developed a list summarizing the selection criteria for PCMs:

- High latent heat of phase change per unit volume and mass and heat capacity in order to allow the most compact system possible.
- Transition temperatures in the temperature range of the target application. For thermal comfort, this range is between 15°C and 30°C [22]. This temperature can be chosen considering the average day and night temperature and other weather conditions [17,36].
- High thermal conductivity to accelerate the charge and discharge of the storage system.
- Low vapour pressure to avoid evaporation that could affect the integrity of the system and reduce its efficiency.
- Low undercooling degree and high crystallization rate to facilitate the charge and discharge of the storage system.
- Low volume expansion during melting which implies very close solid and liquid densities.
- Chemical and thermal stabilities over a high number of charge and discharge cycles without altering the material properties and safely (i.e. non-toxic, non-corrosive, non-flammable and non-explosive).
- Use of an abundant and less expensive material to make the technology attractive for widespread use.

Based on these recommendations, capric acid (CA), a fatty acid, supplied from Alfa Aesar with a purity of 99% has been chosen as PCM in this study. The general information of the CA are presented in Table 1.

Fatty Acid	Acronym	CAS Number	Formula	Supplier	Purity * (%)	Melting Temperature
Capric acid (Decanoic acid)	CA	334-48-5	$C_{10}H_{20}O_2$	Alfa Aesar	99	29-33 °C [25,30]

* Purity as given by the supplier.

Table 1. General information about capric acid (CA)

2.1.2 Preparation of shape-stabilized hemp shives/CA composites

The hemp shives used in this study are the Chanvribat provided by Ecohabitat (Ecological Materials for Habitat) with an average density of about 100 kg/m^3. The choice of hemp shives is governed by their high porous structure with a total accessible porosity of 76.67% [37] which is suitable for impregnation process.

To fabricate the form stable hemp shives/CA composite, the vacuum impregnation technique has been used (Figure 1).

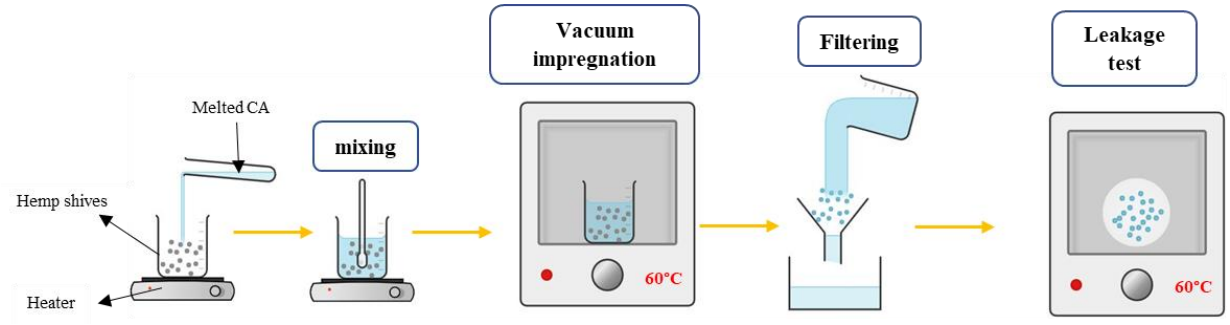

Figure 1. Fabrication of the hemp shives/CA by vacuum impregnation method

Hemp shives (Figure 2.a) are weighed (m_1) and mixed with the pre-weighed liquid CA (Figure 2.b).

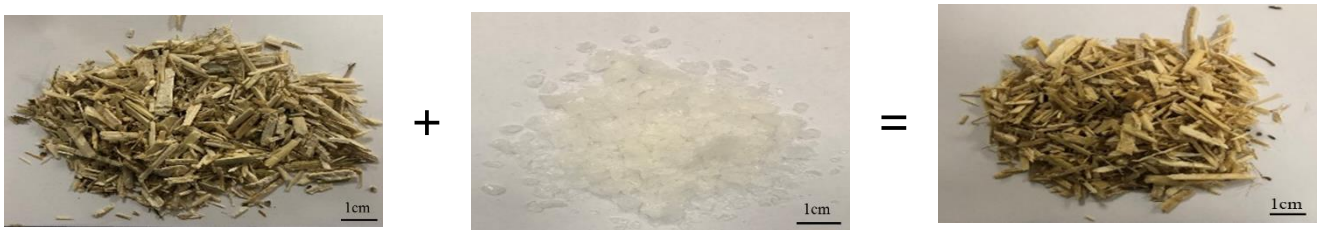

(a) (b) (c)

Figure 2. Images of: (a) hemp shives, (b) CA and (c) form-stable hemp shives/CA composite

The mixture is put in a vacuum oven at a temperature superior to the melting temperature of the PCM (60°C). The melted CA is absorbed in the pores of the hemp shives by capillarity and surface tension forces [38]. The quantity of liquid CA is chosen to recover the hemp shives in order to ensure effective impregnation. The mixture is kept alternatively under vacuum (100 mbar [39]) and non-vacuum conditions to push out the remaining air in the pores of the hemp shives and enhance the diffusion of CA. After the impregnation, the excess of liquid CA is removed by filtration. The impregnated hemp shives are placed on a filter paper and kept on the oven at 60°C to remove the CA at the surface of the hemp shives. The filter paper was changed continually until no leakage was observed. The final mass of the composite (m_2) is weighed and the mass ratio of CA in the composite is calculated using equation (1) according to [38]. The final mass ratio without leakage is 53%. This value is comparable with the value reported in the literature for vegetable fibers: 52% for wood fibers/CA-SA [40], 43-54% for biochar/methylpalmitate [41] and 40.5% for kapok fibers/MA-TD (1-Tetradecanol) [39].

$$R = \frac{m_2 - m_1}{m_2} * 100 \quad (1)$$

2.1.3 Fabrication of hemp concrete PCM

The formulation, which will be used as reference concrete (REF) in the following, has been set in accordance with the professional rules for the execution of hemp products that were definitively validated in 2012. The formulation of hemp concrete consists in mixing 16% hemp shives, 34% tradical® PF40 used as a binder and 50% water.

The manufactured hemp concrete samples (PCM and REF) were conserved for four days in their moulds in a climatic chamber regulated at a temperature (T) of 20 °C and a relative humidity (RH) of 50%. Then, the moulds were disassembled to allow the drying of samples.

For each characterization, two different samples has been fabricated: one acting as a reference (without PCM) and the other one made of shape-stabilized hemp shives/CA with 53% of impregnation rate. Thus, two samples of each (with and without PCM) with dimensions of 15×15×5 cm^3, 10×10×6 cm^3, 5×5×5 cm^3 and 10×10×8 cm^3 are made for thermal conductivity, MBV and thermal performances test respectively.

2.2 Characterization

2.2.1 Morphology and micro-structure

The characterization of the morphology and the microstructure of the samples is essential to understand the impregnation mechanism. The microstructure of the CA, hemp shives and the shape-stabilized hemp shives/CA has been observed successively by scanning electron microscope (SEM) (QUANTA 200 Environmental Field Effect Gun apparatus, FEI, FRANCE) in the environmental mode. This mode avoids any previous treatment of the samples like gold deposit, which could considerably alter the observations. In addition, this mode is very adequate for non-conductive samples like hemp shives. The observations were performed at low pressure (typically 2 mbar), two different voltages (5 for CA and 15 KV for hemp shives) and at different magnifications (70, 500, 600, 2000 and 2400x).

2.2.2 Hygrothermal properties

2.2.2.1 Hygroscopic properties

The hygroscopic properties of the hemp concrete are investigated by measuring the Moisture Buffer Value (MBV). The moisture buffering is the ability to naturally regulate relative humidity through their moisture capacity. Therefore, the MBV quantifies the amount of moisture that a material can store and release when it is subjected to cyclic variations of the surrounding relative humidity (RH) [42]. In this study, the measurement of the MBV has been performed according to the Nordtest Project protocol [43]. Based on this protocol, the hemp concrete samples of dimension 10×10×5 cm^3 are initially preconditioned at 50% RH and 23°C, then exposed to cyclic step-changes in RH between high (75%) and low (33%) values for 8 and 16 hours respectively (Figure 3). The mass of the sample is recorded at each step and used to calculate the MBV according to equation (2):

$$MBV = \frac{\Delta m}{A * (RH_{max} - RH_{min})} \quad (2)$$

Where MBV [g/ (%RH.m^2)] is the Moisture Buffer Value, Δm [g] is the mass variation during the absorption/desorption phase, A [m^2] is the exposed sample surface area and RH_{max}, RH_{max}[%] is the maximum and minimum relative humidity applied during the humidification and drying cycle, respectively.

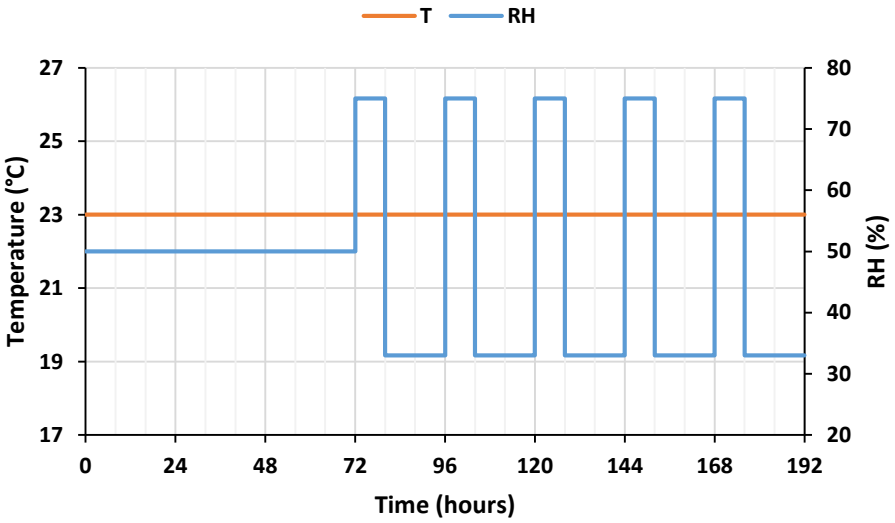

Figure 3. Nordtest Project protocol for the measurement of the MBV

2.2.2.2 Thermal conductivity

Thermal conductivity of the hemp concrete is measured using the λ-Meter Ep500e® device based on the guarded hot plate method under stationary conditions at three different temperatures: 10, 23 and 40°C according to the standard NFEN12664 [44] and NFEN12667 [45]. The dimensions of the hemp concrete samples are 15×15×5 cm^3 and the measurements are performed for both REF and PCM hemp concrete (Figure 4). For each sample, the measurements are conducted three times to verify the repeatability. Since the measurement were conducted three times, the average thermal conductivity ($\bar{k}$) is used and the uncertainty is calculated by using the standard deviation (σ) expressed by the equation (3) :

$$\sigma = \sqrt{\frac{\sum_{i=1}^{n}(k_i - \bar{k})^2}{n-1}} \quad (3)$$

where n is the number of measurement and $\bar{k}$ the average thermal conductivity.

(a) (b)

Figure 4. (a) REF and (b) PCM hemp concrete samples for the thermal conductivity measurement

2.2.2.3 Phase change properties and thermal stability

A DSC3+/TGA differential scanning calorimeter / thermo-gravimetric analyser device provided by METTLER TOLEDO is used to measure the heat flow released by the materials tested as well as the mass change during the tests. TGA is performed to verify the thermal stability of the composite-PCM in the building application temperature range. The long term stability of the composite will be investigated in a future work.

The DSC gives the melting/solidification temperatures and enthalpies of the different samples: CA and hemp shives/CA composites. The DSC was calibrated using four calibration standards (gold, zinc, aluminium and indium) to ensure precise certainty on the temperature range considered. The purity of all the calibration standards is about 99.999%. The melting properties and the uncertainty range of the calibration standards are presented in Table 2. Prior to the measurements, a blank run is performed to correct the baseline. The measurements are performed over a cycle with a heating/cooling rate of 0.5°C.min^{-1} in a range of temperatures from 5 to 40°C for the heating phase, and from 40 to 5°C for the cooling phase (Figure 5). The isothermal steps are hold for 15 minutes in order to avoid the thermal gradient inside the sample [46]. For each sample (CA and hemp shives), a mass between 5 and 20 mg is weighed and placed in 70 µL alumina crucibles. The experiment was carried out by purging the sample cell with Argon at a flow rate of 20 ml.min^{-1}.

The tests are repeated three times for each sample to ensure accuracy and calculate the standard deviation. The integrated software of METTLER TOLEDO is used to calculate the latent heats of fusion and solidification by numerical integration of the area under the peaks that represent the solid-liquid and the liquid-solid phase transitions. The onset temperature is chosen as melting temperature for the fusion peak whereas the endset is selected as solidification temperature for the crystallization peak (Figure 6). These two values are chosen because they are not influenced by the heating rate unlike the peak temperature.

	Literature values		**Standards specifications**		
Material	T (°C)	$\Delta H_m\ (Jg^{-1})$	$\Delta T_s(°C)$	$\Delta T_r(°C)$	$\Delta(\Delta H_m)$ (%)

Indium	156.6	28.45	1.5	2.5	15
Zinc	419.5	107.5	2	3	15
Aluminium	660.3	397	2.5	3.5	20
Gold	1064.2	63.7	3	4	20

Table 2. Melting properties and specifications of the calibration standards, provided by METTLER TOLEDO. T: temperature,H_f: heat of fusion ,ΔT_s: uncertainty on sample temperature, ΔT_r: uncertainty on reference temperature, ΔH_f: uncertainty on heat of fusion

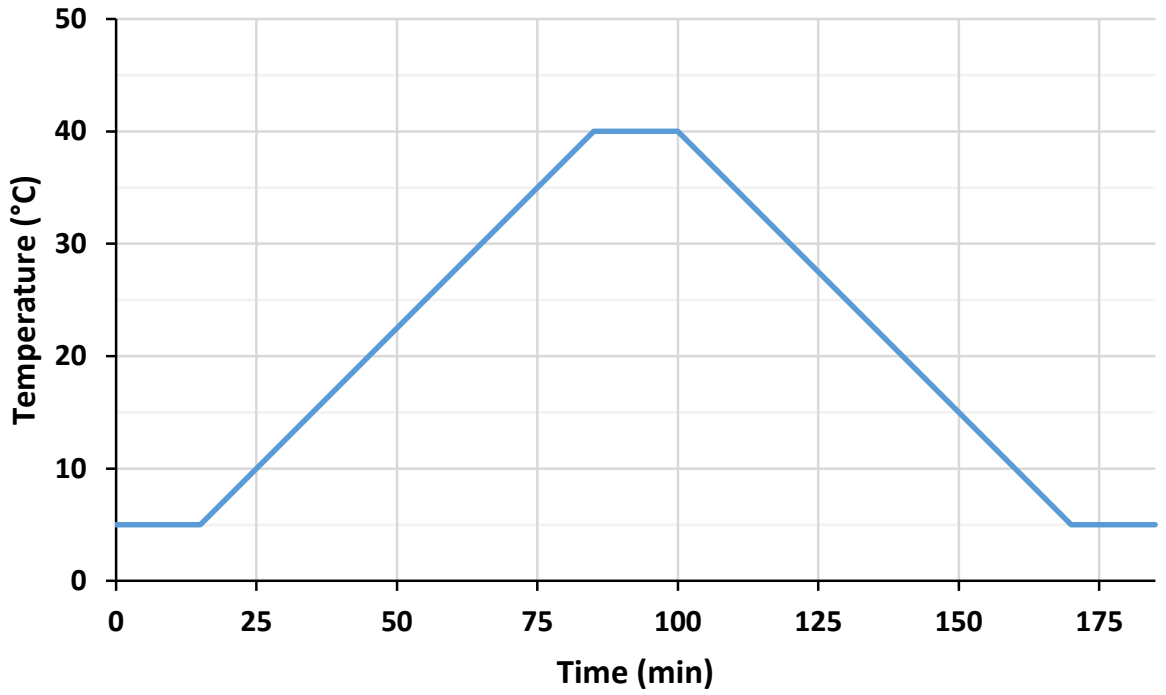

Figure 5. Heating/cooling program for the DSC measurement

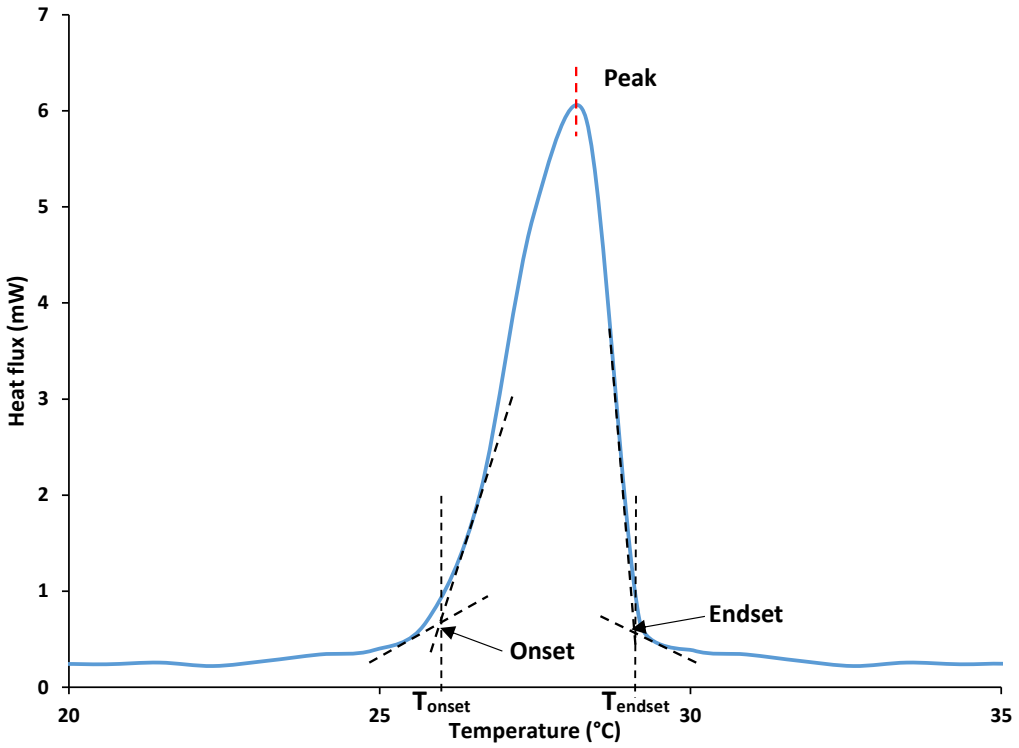

Figure 6. Determination of the onset, endset and peak temperature for exothermic process DSC measurements

The thermogravimetric analysis (TGA) is performed simultaneously with DSC tests on the same sample. TGA allows analysing the thermal stability of the composite in the building temperature's range by quantifying the mass variation of the material according to temperature. CA, hemp shives only and hemp shives/CA composites samples are analysed in a temperature range of 25-500°C with a heating rate of 5°C.min^{-1}. As for the DSC measurements, the tests are also repeated three times for each sample to verify repeatability and reproducibility.

2.2.3 Thermal performances

The thermal performances test are performed in a climatic chamber. This climatic chamber allows the regulation of the temperature and the RH in the working range specified in Table 3.

Temperature range (°C)	**Heating rate range (°C.min^{-1})**	**RH range (%)**
-70 to 180	0.5 to 35	+10 to +90

Table 3. Temperature, heating rate and RH ranges of the climatic chamber

REF and the PCM hemp concrete of dimension 10×10×8 cm^3 are placed in the climatic chamber and subjected to temperature variations between 5 and 40°C at 50% of relative humidity. In order to ensure a unidirectional moisture flow from only one side of the cube, the tested samples are covered by aluminium foil on 5 sides (Figure 7). As the targeted application is passive latent heat storage, diurnal temperature variation is applied. The latter means that the temperature varies between minimum and maximum values within 24 hours (Figure 8). Measurements are

performed for 7 days, including a 3-day preconditioning at 23°C and 50% relative humidity to ensure testing under fixed humidity conditions.

Figure 7. REF and PCM hemp concrete samples for the thermal performances test and the position of the RH and T sensors

In order to record the temperature inside the hemp concrete, the temperature and RH sensors (Ahlborn FHA 646 R) are used and placed at three different positions (2.5, 5 and 7.5 cm) and at the same depth (5 cm) as presented in Figure 7. The RH measurement circuit is capacitive, while an N-type thermistor is used to measure temperature. The advantages of these captors is their small size and the measurement of both temperature and RH. The sensors were pre-calibrated by the manufacturer. They are connected to the ALMEMO data acquisition system that records the data every minute. The technical specifications of the sensors are presented in Table 4.

RH accuracy	±2%
T accuracy	−2 0 to 0°C : ±0.4°C ; 0 to 70°C : ±0.2°C : 70 to 100°C : ±0.6°C
RH measurement range	0 to100 % RH
T measurement range	− 20 to100 °C
Maximum response time	10 s

Table 4. Technical specifications of the RH and T sensors

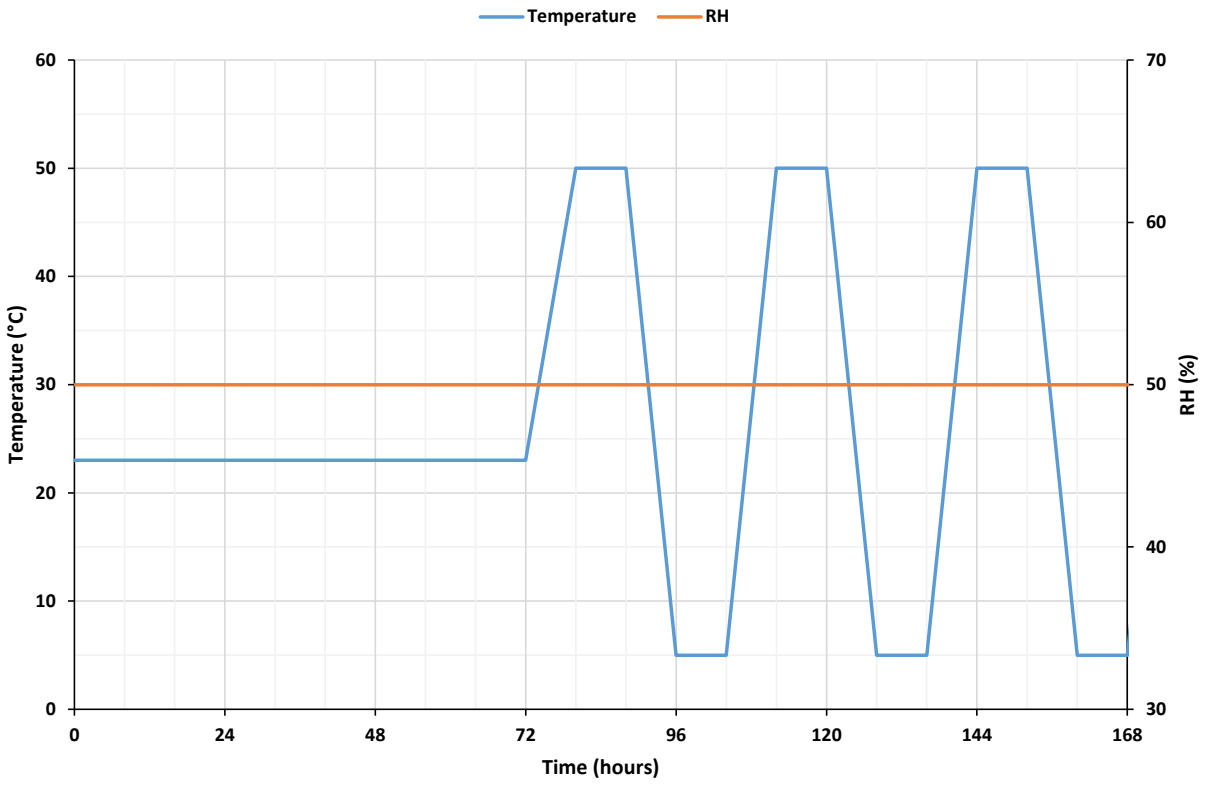

Figure 8. Temperature program for the thermal performances test in the climatic chamber

3 Results and discussion

3.1 Characterization of form-stable hemp shives/CA composites

3.1.1 Morphology and microstructure

Figure 9 and Figure 11 shows the SEM images of pure CA (Figure 9.(a,b)), melted and recrystallized CA (Figure 9.(c,d)), hemp shives only (Figure 11.a) and hemp shives/CA composite (Figure 11.(b,c,d)) at different magnifications and voltage. For CA it was impossible to work at high voltage because the sample melts instantaneously. This phenomenon is inherent to the relative low melting temperature of CA (approximately 30°C).

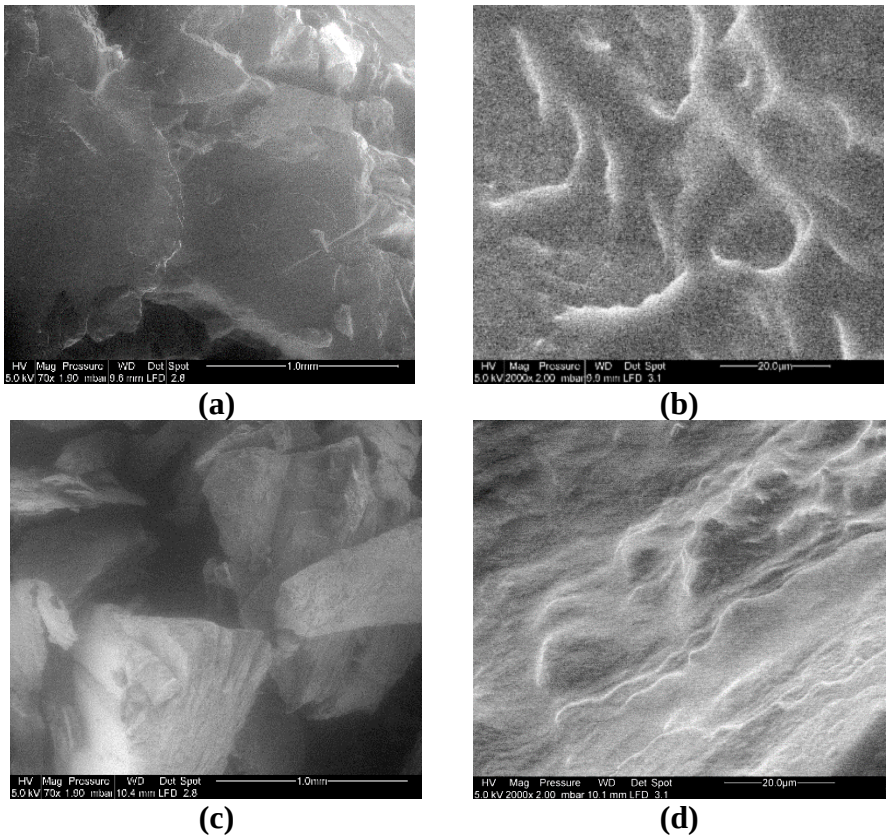

Figure 9. SEM images of: (a,b) pure CA, (c,d) melted and recrystallized CA at 70 and 2000x magnifications

The pure CA presents a regular shaped-crystal structure as observed by [40] (Figure 9.a). The size of the crystals is increased after melting and solidification and the structure is more regular, indeed, a paste-like texture is observed (Figure 9.d). At first sight, we can notice that the melting/crystallization process increases the crystallinity of the capric acid. Morover, the CA was more electron conductor and easier to study by SEM due to increased crystallinity [47,48]. The energy dispersive spectroscopy (EDS) spectra obtained for CA (Figure 10) is in adequation with the results based on the chemical composition of CA. From the EDS spectrum of CA, we observed that the mass fraction of O is 19.8% against 80.1% for C and H. It should be recalled that EDS does not detect the transitions of H and their contribution is reported in that of C.

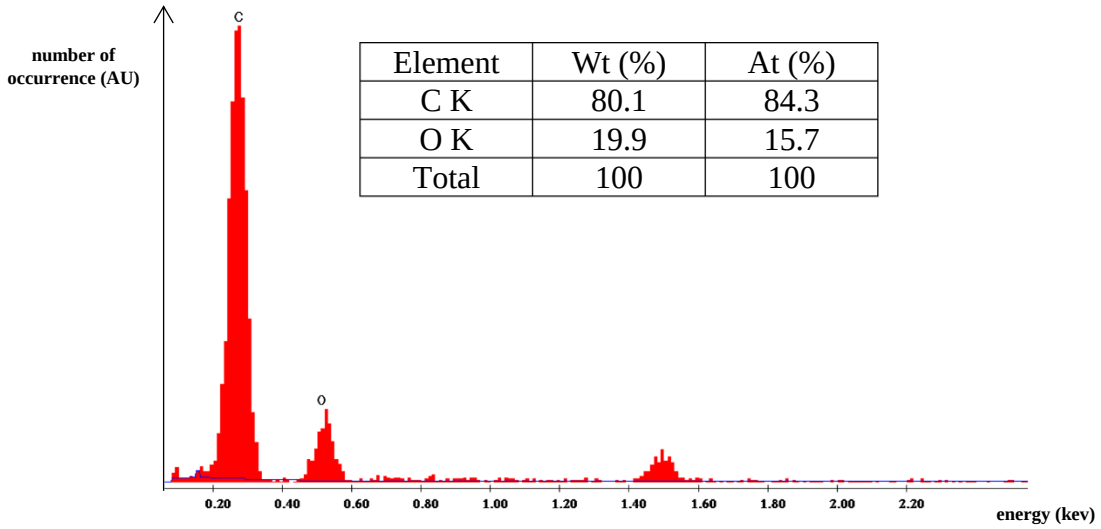

Element	Wt (%)	At (%)
C K	80.1	84.3
O K	19.9	15.7
Total	100	100

Figure 10. EDS spectra and composition of CA

The cross section images of the pure hemp shives (Figure 9.a) shows a very porous structure. As stated in the literature, the pores are approximately 50–80 µm in diameter and are surrounded by relatively thick cell walls which are mainly composed of cellulose, hemicellulose, lignin and pectin [37]. Figure 11.(b,c,d) show the form stable hem shives/CA and that the pores of the hemp shives are successfully occupied by CA after the vacuum impregnation process by means of physical absorption. The CA is trapped without leakage in the microstructure of hemp shives thanks to hydrogen bond attraction, capillary and surface tension forces [40].

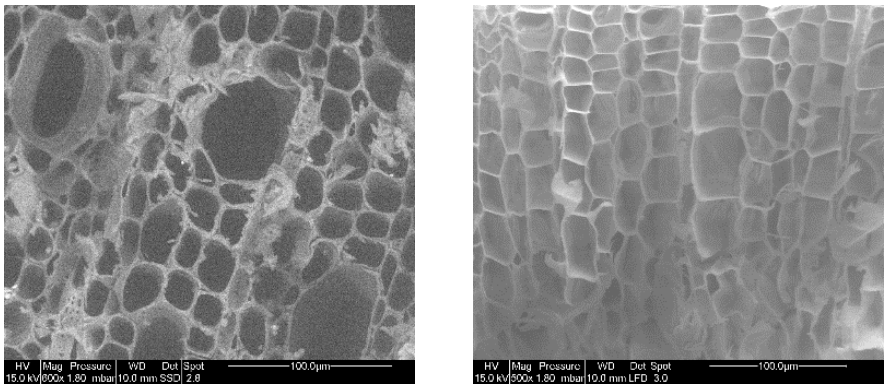

(a) **(b)**

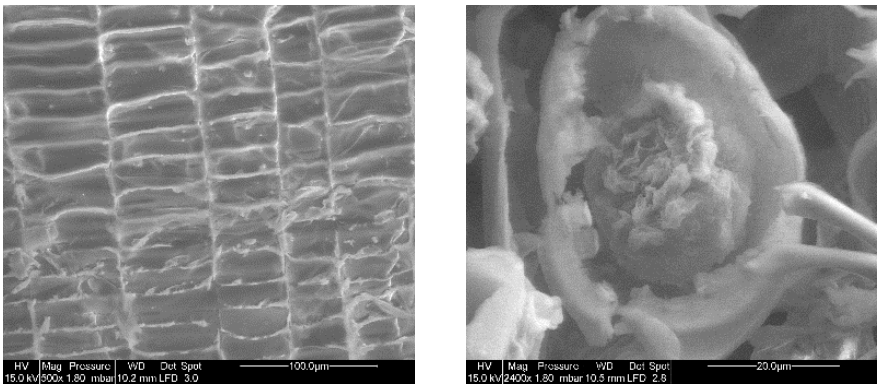

(c) **(d)**

Figure 11. SEM images of: (a) hemp shives, (b,c,d) form stable hemp shives/CA at respectively 500x and 2400x magnifications.

3.1.2 Phase change and thermal properties

3.1.2.1 DSC

DSC is used to measure thermal energy storage capacity through investigation of the melting/solidification properties of the prepared PCM composite. Figure 12 shows the DSC curve of the CA, hemp shives and hemp shives/CA composite. The melting and solidification temperatures and the enthalpies of the different materials are presented in Table 5 with the uncertainty associated. As mentioned in section 2.2, the onset temperature is chosen for endothermic processes whereas the endset temperature is used for exothermic processes. The melting and solidification temperatures of CA and hemp shives/CA composite were obtained as 29.8±0.1 °C and 25±1 °C, 28.9±0.4 °C and 23±1 °C, respectively. The enthalpies of melting and solidification were calculated as 140.7±3.1 and 135.6±2.6 $J.g^{-1}$, 78.7±4.6 and 76.4±3.1 $J.g^{-1}$, respectively.

As can be seen, the measured melting and solidification temperatures and enthalpies for CA are consistent with the values provided by the literature [25]. Both melting/solidification enthalpies are reduced after the fabrication of the shape-stabilized hemp shives/CA composite. This reduction is caused by the reduction of the mass ratio of CA in the composite and the reduction of the crystallinity of the CA. Additionally, the melting/solidification temperatures are lower compared to pure CA before impregnation. This decrease in phase change temperatures can be due to weak attractive interaction between fatty acid molecules and inner surface wall of the porous material [26].

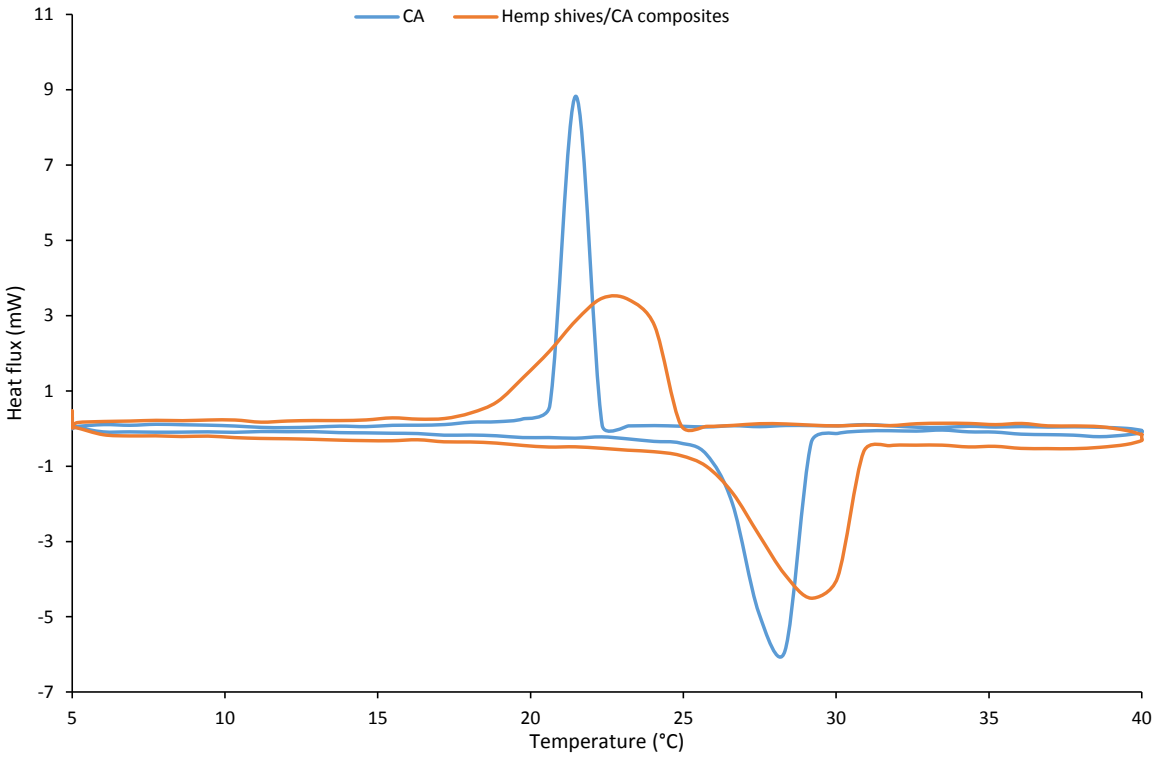

Figure 12. DSC curves of CA, hemp shives only and hemp shives/CA composite

Samples	Melting process			Solidification process		
	T_m(°C)	T_{peak}(°C)	ΔH_m(J.g^{-1})	T_s(°C)	T_{peak}(°C)	ΔH_s(J.g^{-1})
CA	29.8±0.1	30.4±0.1	140.7±3.1	25±1	26.8±0.9	135.6±2.6
Hemp shives/CA	28.9±0.4	31.6±0.2	78.7±4.6	23±1	27.3±0.4	76.4±3.1

Table 5. Melting/solidification temperatures and enthalpies of CA and hemp shives/CA composite

The measured latent heats of melting and solidification of the composite PCMs were close to the values calculated by multiplying the mass ratio of the CA in the composites, and their phase change enthalpies as stated by [49]. In fact, the ratio of the heat of fusion of pure CA and hemp shives/CA is 56% that is very close to the theoretical value of the impregnation rate (53%).

Although the latent heats of the prepared hemp shives/CA composite decreased significantly due to shape stabilization, these latent heat values are still very promising for energy storage in buildings compared to shape-stabilized PCMs studied by other references, as listed in Table 6.

PCM composites	Melting temperature (°C)	Solidification temperature (°C)	Heat of fusion (J.g^{-1})	Heat of solidification (J.g^{-1})	Reference
Wood flour/paraffin	26.18	-	20.62	-	[50]
Wood flour/CA-PA	22.03	20.06	28.16	29.77	[51]
Wood	23.38	21.87	92.1	91.9	[40]

fiber/CA-SA					
Kapok fibers/MA-TD	24-42.3	10.5-29.7	76.8	77.4	[39]
Hemp shives/CA	**28.9±0.4**	**23±1**	**78.7±4.6**	**76.4±3.1**	**This study**

Table 6. Comparison of the phase change properties of the prepared hemp shives/CA composite with that of some bio-based PCM composites

3.1.2.2 TGA/DTG

TGA/DTG is essential in order to ensure the stability of the materials on the temperature range of buildings. The TGA measures mass changes in a material as a function of temperature (or time) under a controlled atmosphere. The first derivative of the TGA curve (the DTG curve) helps to determine inflection points, useful for further interpretation as well as for differential thermal analysis. Figure 13 and Figure 14 show respectively the weight loss and derivated thermogravimetry (DTG) curve of CA, hemp shives only and hemp shives/CA form-stable composite from room temperature (25°C) to 500°C.

From the different curves, it can be seen that CA is mainly degraded between 150 and 240°C with degradation starting at around 125°C. This observation is in adequation with the results obtained by Kar et al. [52].

Concerning hemp shives only, the DTA curve shows a first peak between 50 and 150°C attributed to the evaporation of free water in the hemp shives. A second degradation shoulder peak at about 250-335°C is attributed to thermal depolymerisation of hemicelluloses or pectin. The final decomposition peak occurring between 300 and 380°C is attributed to the decomposition of cellulose [53].

The TGA curve of the form stable hemp shives/CA is a superposition of the weight loss curve of CA and hemp shives. The same phenomena are observed at the same temperature. From the DTG curve that allows detecting the temperature at which transformations occur, it is found that the form stable composite exhibits good thermal stability under 170°C with less than 10% of mass loss making it suitable for building application for which the temperature rarely exceeds 60°C. TGA is also a way to obtain the impregnation rate of the hemp shives/composite and correct the theoretical value if needed. From the TGA curve, the impregnation rate is approximately 53.97%, which is in accordance with the theoretical value found (53%). The discrepancies are explained by the statistical behaviour of the impregnation process (all the particles will not absorb the same amount of CA) and the error induced by the sampling.

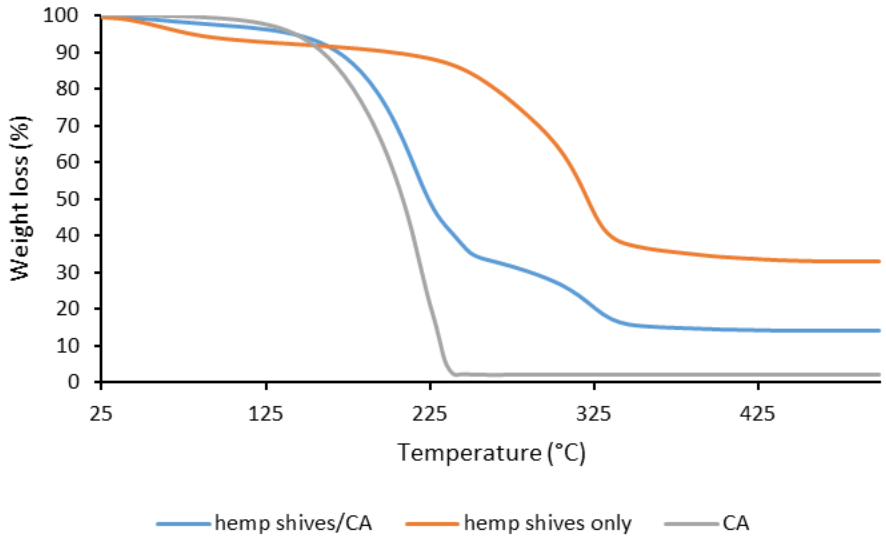

Figure 13. TGA curves of CA, hemp shives only and the fabricated form stable hemp shives/CA

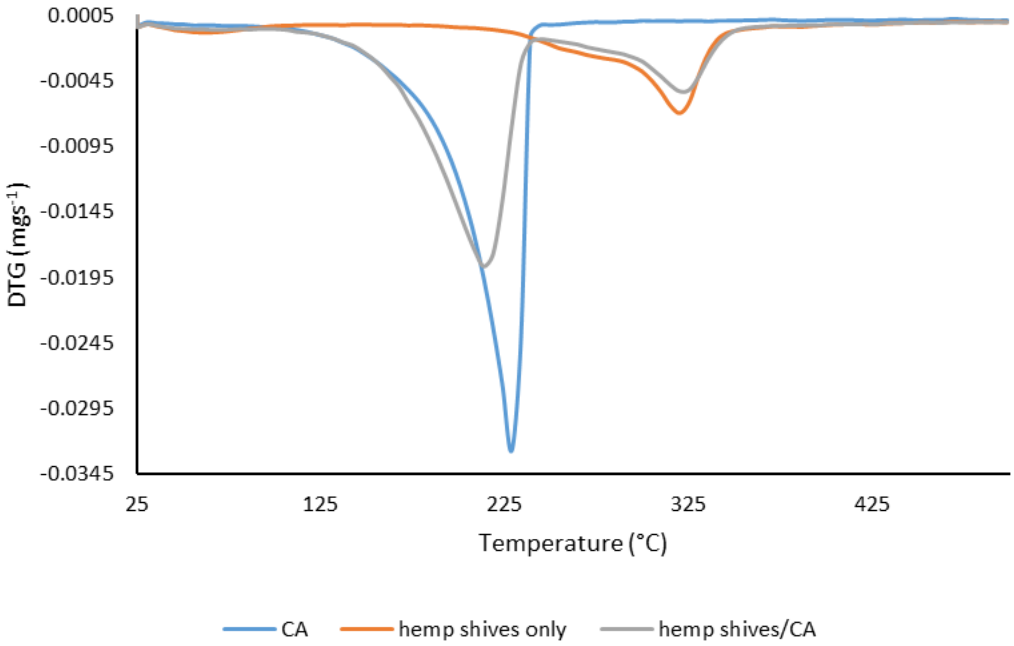

Figure 14. DTG curves of CA, hemp shives only and the fabricated form stable hemp shives/CA

3.2 Hygrothermal properties of hemp concrete PCM

3.2.1 Thermal conductivity

Thermal conductivity is one of the key parameters that is considered in the selection of materials for building application. Thermal conductivity measures the rate at which temperature gradient transmits through a material. It allows to classify of materials as isulators or conductors and thus to select a material for a specific application. The results of the thermal conductivity of REF and PCM hemp concrete composite and the uncertainty associated is presented at three different temperatures (10, 23 and 40°C) in Figure 15. For each sample, the thermal conductivity was 0.084, 0.088 and 0.094 $Wm^{-1}K^{-1}$ for PCM hemp concrete compared to 0.066, 0.07 and 0.075 $Wm^{-1}K^{-1}$ for the REF at 10, 23 and 40°C respectively. According to Arnaud et al. [54], the thermal conductivity of hemp concrete varies between 0.06 and 0.18 $Wm^{-1}K^{-1}$ for a dry density ranging from 200 to 800 $kg.m^{-3}$, which is in accordance with the values measured in this study.

As noted, the thermal conductivity of hemp concrete increases with the addition of CA. Indeed, increases in thermal conductivity of 27%, 26% and 25% are observed for PCM hemp concrete compared to REF at 10, 23 and 40°C respectively. This result was expected according to the literature of shape-stabilized PCMs where the thermal conductivity of the porous support is enhanced by the impregnation with PCMs [7,19,55–57]. The reason is that the thermal conductivity of the composite PCM is higher than that of the corresponding support matrix, because CA has replaced air in the hemp shives/CA composites. The thermal conductivity of CA (about 0.21 $Wm^{-1}K^{-1}$ at ambient temperature [25]) is 10 times higher than that of air (about 0.02 $Wm^{-1}K^{-1}$).

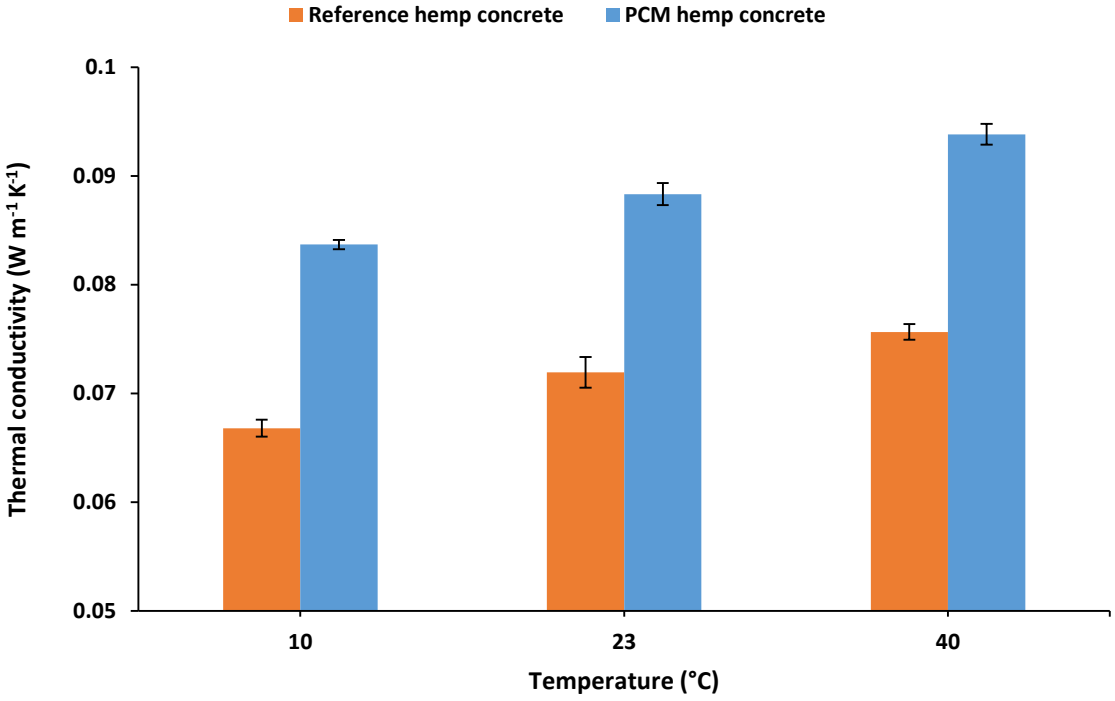

Figure 15. Thermal conductivity of reference and PCM hemp concrete at 10, 23 and 40°C.

3.2.2 MBV

The MBV is used to estimate the dynamic hygrothermal behavior of the material when exposed to an indoor environment. It indicates the average amount of water that is exchanged by sorption or desorption when the material surfaces are subjected to relative humidity variations over a given time. The MBV values were calculated as 3.05±0.34 and 2.23±0.23 $g.m^{-2}.\%RH^{-1}$ for REF and PCM hemp concrete respectively, according to the Nordtest program protocol. The MBV of REF is in agreement with the results of [58] where the average MBV for a hemp concrete varied between 1.82 $g.m^{-2}.\%RH^{-1}$ and 3.02 $g.m^{-2}.\%RH^{-1}$. The results show a reduction of the MBV with the incorporation of the PCM. This result is due to the reduction of the absorption of the hemp shives with the incorporation of the PCM. Despite the decrease in the MBV, both REF and PCM hemp concrete are classified as excellent humidity regulator regarding the classification of Nordtest Project (Figure 16).

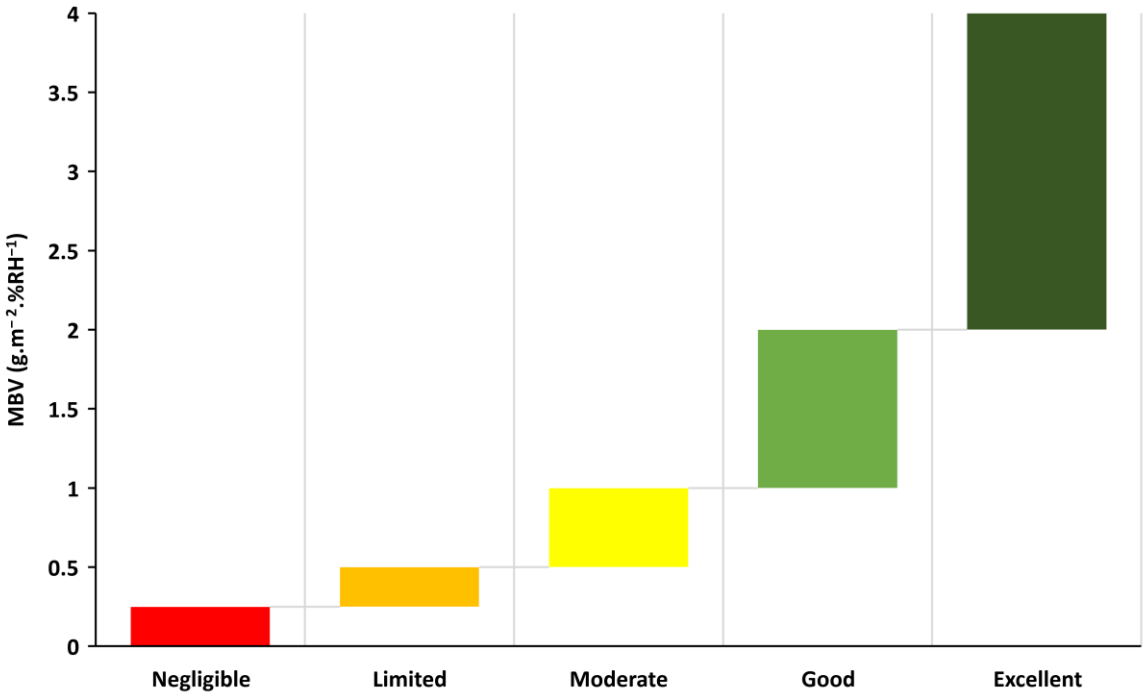

Figure 16. Classification of the MBV according to Nordtest project

3.3 Thermal performances of hemp concrete PCM

The thermal performances of the PCM hemp concrete and REF submitted to cyclic temperature variations between 5 and 50°C have been investigated in a climatic chamber for 7 days. Figure 17 shows the temperature evolution in REF and PCM hemp concrete composite as well as the temperature in the climatic chamber. It can be seen that the temperature recorded by the three sensors in each sample are almost identical. The standard deviation is about 0.1°C and 0.2°C for REF and PCM hemp concrete, which is in the uncertainty range of the sensor (0.2°C).

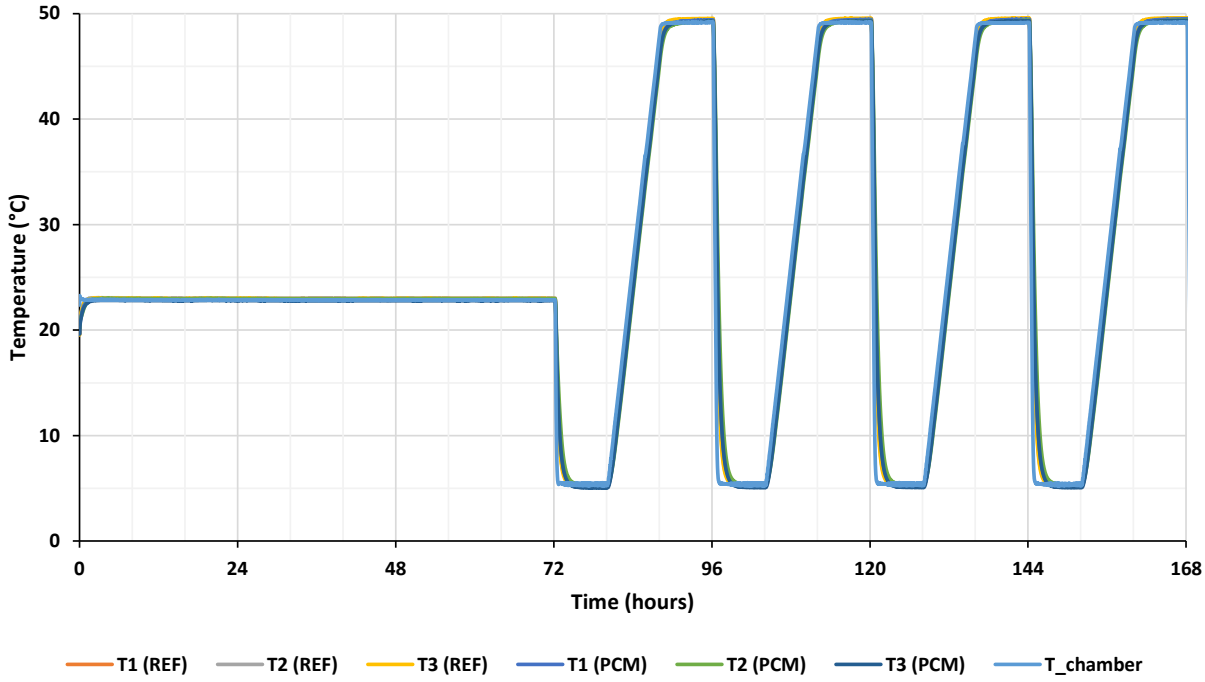

Figure 17. Evolution of the temperature of the reference and PCM hemp concrete for the different T sensors.

Figure 18 shows the evolution of the average temperature of the three sensors placed in each sample (REF and PCM hemp concrete) over a 24-hour cycle. Three phases can be distinguished: an ascending phase, a stabilization phase and a descending phase. During the ascending phase, the temperature of the PCM hemp concrete is slightly lower than for REF. The trend is reversed during the descending phase over which the temperature of the PCM hemp concrete remains slightly higher than REF. This difference is explained by the LHTES effect of PCM hemp concrete as well as the sensible heat absorption that delays the increase or decrease in the temperature in the sample [59].

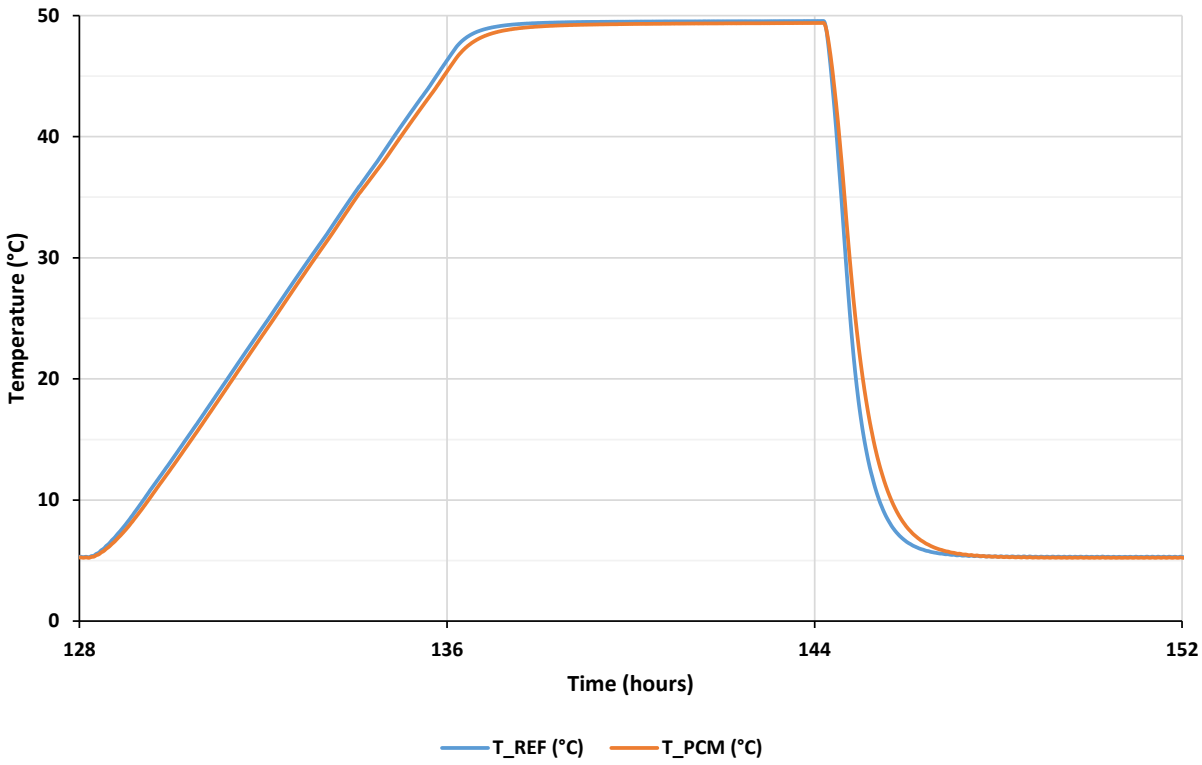

Figure 18. Evolution of the aerage temperature of the reference and PCM hemp concrete within a 24-hour cycle

To further quantify the temperature difference between REF and the PCM hemp concrete, we have plotted the evolution of the temperature difference (ΔT) between REF and PCM hemp concrete over time (Figure 19). The maximum difference is about 1°C during the heating phase against 4.6°C for the cooling phase. The difference for the cooling phase is particularly pronounced in the temperature range 5-30 °C. This result indicates that the PCM hemp concrete is more efficient during cooling periods. This is due to the fact that PCM discharges and releases its latent heat stored during heating periods inside the PCM hemp concrete sample preventing the temperature of the hemp concrete to drop immediately. The maximum time shift for the heating and the cooling period are 30 minutes and 20 minutes, respectively. These experimental results showed the good thermoregulation capacity of the PCM hemp concrete.

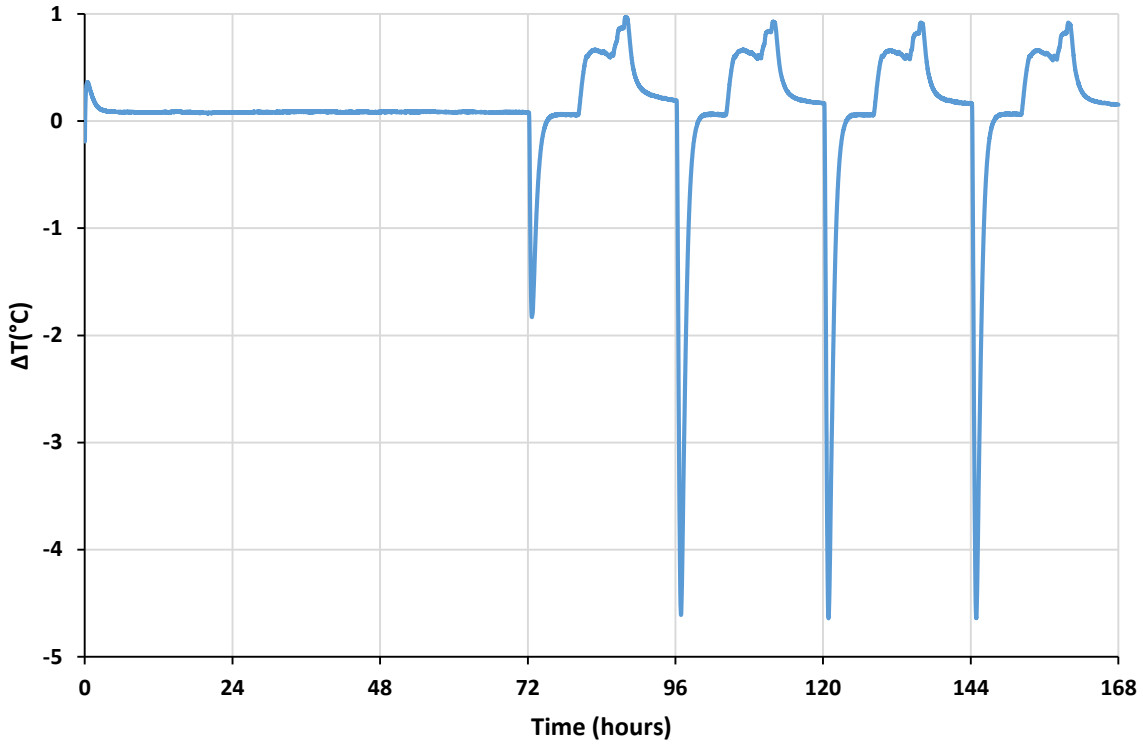

Figure 19. Evolution of the temperature difference between the reference and PCM hemp concrete

4 Conclusion

This study investigated the hygrothermal performances of a novel PCM hemp concrete for passive thermal energy storage in buildings. CA for his suitable melting properties and renewable origin has been used to fabricate shape-stabilized hemp shives/CA composite using vacuum impregnation technique. The principal findings of this study are presented as follow:

- CA was successfully impregnated in hemp shives with 53% incorporation rate without any leakage. This observation was confirmed by SEM results, which showed that the CA was efficiently retained in the porous structure of the hemp shives.
- DSC results showed that the hemp shives PCM composite possess promising melting and solidification properties. The melting and solidification temperatures of CA and hemp shives/CA composite were obtained as 29.8°C and 25 °C, 28.9°C and 23±1 °C, respectively. The enthalpies of melting and solidification were calculated as 140.7 and 135.6 $J.g^{-1}$, 78.7 and 76.4 $J.g^{-1}$, respectively. These results indicated a reduction of the latent heat of the PCM composite compared to the pure PCM. However, these values are still very promising for energy storage in buildings compared to shape-stabilized PCMs studied by other references. The TGA/dTG results indicated that the form stable composite exhibits promising thermal stability under 170°C making it suitable for building application.

- The shape-stabilized hemp shives/CA composite is used to fabricate PCM hemp concrete. The hygrothermal properties of the PCM hemp concrete are assessed and compared to REF. The thermal conductivity measurement conducted at three temperatures (10, 23, 40°C) indicated an increase in the thermal conductivity (of about 25.7% at 23°C) of the PCM hemp concrete compared to REF.
- The moisture buffer value (MBV) is defined as the capacity of the material to regulate the humidity. The MBV of the PCM hemp concrete and REF are measured following the Nordtest protocol. The MBV values were 3.05 and 2.23 $g.m^{-2}.\%RH^{-1}$ for REF and the PCM hemp concrete respectively which allow classifying them as excellent humidity regulator regarding the classification of Nordtest Project.
- The thermal performances test conducted in a climatic chamber showed that the PCM hemp concrete present promising thermoregulation capacity. The maximum temperature difference between REF and PCM hemp concrete and time shift were about 1°C and 30 minutes during the heating phase against 4.6°C and 20 minutes for the cooling phase.

Further study should be conducted to determine the long-term stability and cyclability of the hemp shives/CA and the PCM hemp concrete. Different temperature programs with realistic weather can be tested in order to investigate the behaviour of the PCM hemp concrete under various conditions. Finally, a real scale-cycling thermal performance at the building envelope scale should be also investigated.

Author Contributions: Conceptualization, all authors; methodology, all authors; formal analysis, all authors; investigation, all authors; resources, all authors; data curation, all authors; writing—original draft preparation, M.S.; writing—review and editing, all authors; visualization, all authors; supervision, R.B., M.D., and A.H.; project administration, R.B. and M.D.; funding acquisition, R.B., M.D. All authors have read and agreed to the published version of the manuscript.

Declaration of Competing Interest: The authors declare that they have no known competing financial interests or personal relationships that could have appeared to influence the work reported in this paper.

Acknowledgments: The authors are grateful to the Region Nouvelle Aquitaine for subsidizing BioMCP project (Project-2017-1R10209-13023) and Energy saving certificate program of the Ministry of Ecological and Solidarity Transition 'SmartReno support" 2019–2021. The authors would like also to thank Dr. Egle CONFORTO, responsible of the electron microscopy platform of the LaSIE laboratory of La Rochelle University for the technical assistance in SEM acquisition.

References

[1] Buildings – Topics, IEA. (n.d.). https://www.iea.org/topics/buildings (accessed April 30, 2021).

[2] V. Masson-Delmotte, P. Zhai, A. Pirani, S.L. Connors, C. Péan, S. Berger, N. Caud, Y. Chen, L. Goldfarb, M.I. Gomis, M. Huang, K. Leitzell, E. Lonnoy, J.B.R. Matthews, T.K. Maycock, T. Waterfield, Ö. Yelekçi, R. Yu, B. Zhou, eds., Climate Change 2021: The

Physical Science Basis. Contribution of Working Group I to the Sixth Assessment Report of the Intergovernmental Panel on Climate Change, Cambridge University Press, 2021.
[3] V. Basecq, G. Michaux, P. Blondeau, C. Inard, Short term storage systems of the thermal energy for buildings: a review, Advances in Building Energy Research. 7 (2013) 66–119. https://hal.archives-ouvertes.fr/hal-01052828 (accessed May 5, 2021).
[4] K. Sergei, C. Shen, Y. Jiang, A review of the current work potential of a trombe wall, Renewable and Sustainable Energy Reviews. 130 (2020) 109947. https://doi.org/10.1016/j.rser.2020.109947.
[5] M.M. Farid, A.M. Khudhair, S.A.K. Razack, S. Al-Hallaj, A review on phase change energy storage: Materials and applications, Energy Conversion and Management. 45 (2004) 1597–1615. https://doi.org/10.1016/j.enconman.2003.09.015.
[6] M. Jafaripour, S.M. Sadrameli, H. Pahlavanzadeh, S.A.H.S. Mousavi, Fabrication and optimization of kaolin/stearic acid composite as a form-stable phase change material for application in the thermal energy storage systems, Journal of Energy Storage. 33 (2021) 102155. https://doi.org/10.1016/j.est.2020.102155.
[7] P.K.S. Rathore, S.K. Shukla, Enhanced thermophysical properties of organic PCM through shape stabilization for thermal energy storage in buildings: A state of the art review, Energy and Buildings. 236 (2021) 110799. https://doi.org/10.1016/j.enbuild.2021.110799.
[8] S.R.L. da Cunha, J.L.B. de Aguiar, Phase change materials and energy efficiency of buildings: A review of knowledge, Journal of Energy Storage. 27 (2020) 101083. https://doi.org/10.1016/j.est.2019.101083.
[9] R. Baetens, B.P. Jelle, A. Gustavsen, Phase change materials for building applications: A state-of-the-art review, Energy and Buildings. 42 (2010) 1361–1368. https://doi.org/10.1016/j.enbuild.2010.03.026.
[10] B. Lamrani, K. Johannes, F. Kuznik, Phase change materials integrated into building walls: An updated review, Renewable and Sustainable Energy Reviews. 140 (2021) 110751. https://doi.org/10.1016/j.rser.2021.110751.
[11] T. Silva, R. Vicente, F. Rodrigues, A. Samagaio, C. Cardoso, Performance of a window shutter with phase change material under summer Mediterranean climate conditions, Applied Thermal Engineering. 84 (2015) 246–256. https://doi.org/10.1016/j.applthermaleng.2015.03.059.
[12] K.O. Lee, M.A. Medina, X. Sun, X. Jin, Thermal performance of phase change materials (PCM)-enhanced cellulose insulation in passive solar residential building walls, Solar Energy. 163 (2018) 113–121. https://doi.org/10.1016/j.solener.2018.01.086.
[13] U. Berardi, S. Soudian, Experimental investigation of latent heat thermal energy storage using PCMs with different melting temperatures for building retrofit, Energy and Buildings. 185 (2019) 180–195. https://doi.org/10.1016/j.enbuild.2018.12.016.
[14] J. Yu, Q. Yang, H. Ye, Y. Luo, J. Huang, X. Xu, W. Gang, J. Wang, Thermal performance evaluation and optimal design of building roof with outer-layer shape-stabilized PCM, Renewable Energy. 145 (2020) 2538–2549. https://doi.org/10.1016/j.renene.2019.08.026.
[15] A.A.A.A. Al-Rashed, A.A. Alnaqi, J. Alsarraf, Energy-saving of building envelope using passive PCM technique: A case study of Kuwait City climate conditions, Sustainable Energy Technologies and Assessments. 46 (2021) 101254. https://doi.org/10.1016/j.seta.2021.101254.
[16] E. Meng, H. Yu, B. Zhou, Study of the thermal behavior of the composite phase change material (PCM) room in summer and winter, Applied Thermal Engineering. 126 (2017) 212–225. https://doi.org/10.1016/j.applthermaleng.2017.07.110.

[17] H. Akeiber, P. Nejat, M.Z.Abd. Majid, M.A. Wahid, F. Jomehzadeh, I. Zeynali Famileh, J.K. Calautit, B.R. Hughes, S.A. Zaki, A review on phase change material (PCM) for sustainable passive cooling in building envelopes, Renewable and Sustainable Energy Reviews. 60 (2016) 1470–1497. https://doi.org/10.1016/j.rser.2016.03.036.
[18] S. Ali Memon, T. Yiu Lo, X. Shi, S. Barbhuiya, H. Cui, Preparation, characterization and thermal properties of Lauryl alcohol/Kaolin as novel form-stable composite phase change material for thermal energy storage in buildings, Applied Thermal Engineering. 59 (2013) 336–347. https://doi.org/10.1016/j.applthermaleng.2013.05.015.
[19] M.M. Umair, Y. Zhang, K. Iqbal, S. Zhang, B. Tang, Novel strategies and supporting materials applied to shape-stabilize organic phase change materials for thermal energy storage–A review, Applied Energy. 235 (2019) 846–873. https://doi.org/10.1016/j.apenergy.2018.11.017.
[20] M. Sawadogo, M. Duquesne, R. Belarbi, A.E.A. Hamami, A. Godin, Review on the Integration of Phase Change Materials in Building Envelopes for Passive Latent Heat Storage, Applied Sciences. 11 (2021) 9305. https://doi.org/10.3390/app11199305.
[21] A. Abhat, Low temperature latent heat thermal energy storage: Heat storage materials, Solar Energy. 30 (1983) 313–332. https://doi.org/10.1016/0038-092X(83)90186-X.
[22] B. Lamrani, K. Johannes, F. Kuznik, Phase change materials integrated into building walls: An updated review, Renewable and Sustainable Energy Reviews. 140 (2021) 110751. https://doi.org/10.1016/j.rser.2021.110751.
[23] D. Feldman, M.M. Shapiro, D. Banu, C.J. Fuks, Fatty acids and their mixtures as phase-change materials for thermal energy storage, Solar Energy Materials. 18 (1989) 201–216. https://doi.org/10.1016/0165-1633(89)90054-3.
[24] J. Liang, L. Zhimeng, Y. Ye, W. Yanjun, L. Jingxin, Z. Changlin, Fabrication and characterization of fatty acid/wood-flour composites as novel form-stable phase change materials for thermal energy storage, Energy and Buildings. 171 (2018) 88–99. https://doi.org/10.1016/j.enbuild.2018.04.044.
[25] M. Duquesne, C. Mailhé, S. Doppiu, J.-L. Dauvergne, S. Santos-Moreno, A. Godin, G. Fleury, F. Rouault, E. Palomo del Barrio, Characterization of Fatty Acids as Biobased Organic Materials for Latent Heat Storage, Materials. 14 (2021) 4707. https://doi.org/10.3390/ma14164707.
[26] A. Karaipekli, A. Sarı, Preparation, thermal properties and thermal reliability of eutectic mixtures of fatty acids/expanded vermiculite as novel form-stable composites for energy storage, Journal of Industrial and Engineering Chemistry. 16 (2010) 767–773. https://doi.org/10.1016/j.jiec.2010.07.003.
[27] S. Ben Romdhane, A. Amamou, R. Ben Khalifa, N.M. Saïd, Z. Younsi, A. Jemni, A review on thermal energy storage using phase change materials in passive building applications, Journal of Building Engineering. 32 (2020) 101563. https://doi.org/10.1016/j.jobe.2020.101563.
[28] L. Boussaba, A. Foufa, S. Makhlouf, G. Lefebvre, L. Royon, Elaboration and properties of a composite bio-based PCM for an application in building envelopes, Construction and Building Materials. 185 (2018) 156–165. https://doi.org/10.1016/j.conbuildmat.2018.07.098.
[29] M. Duquesne, C. Mailhé, K. Ruiz-Onofre, F. Achchaq, Biosourced organic materials for latent heat storage: An economic and eco-friendly alternative, Energy. 188 (2019) 116067. https://doi.org/10.1016/j.energy.2019.116067.

[30] H. Ke, Phase diagrams, eutectic mass ratios and thermal energy storage properties of multiple fatty acid eutectics as novel solid-liquid phase change materials for storage and retrieval of thermal energy, Applied Thermal Engineering. 113 (2017) 1319–1331. https://doi.org/10.1016/j.applthermaleng.2016.11.158.
[31] F. Benmahiddine, R. Cherif, F. Bennai, R. Belarbi, A. Tahakourt, K. Abahri, Effect of flax shives content and size on the hygrothermal and mechanical properties of flax concrete, Construction and Building Materials. 262 (2020) 120077. https://doi.org/10.1016/j.conbuildmat.2020.120077.
[32] G. Delannoy, S. Marceau, P. Glé, E. Gourlay, M. Guéguen-Minerbe, D. Diafi, I. Nour, S. Amziane, F. Farcas, Aging of hemp shiv used for concrete, Materials and Design. 160 (2018) 752–762. https://doi.org/10.1016/j.matdes.2018.10.016.
[33] B. Seng, S. Lorente, C. Magniont, Scale analysis of heat and moisture transfer through bio-based materials — Application to hemp concrete, Energy and Buildings. 155 (2017) 546–558. https://doi.org/10.1016/j.enbuild.2017.09.026.
[34] K. Abahri, C. El Hachem, F. Bennai, N. Toan, R. Belarbi, Prediction of hemp concrete morphological deformation by x-ray tomography, in: 2017: pp. 616–625.
[35] J. Schröder, K. Gawron, Latent heat storage, International Journal of Energy Research. 5 (1981) 103–109. https://doi.org/10.1002/er.4440050202.
[36] H. Wang, W. Lu, Z. Wu, G. Zhang, Parametric analysis of applying PCM wallboards for energy saving in high-rise lightweight buildings in Shanghai, Renewable Energy. 145 (2020) 52–64. https://doi.org/10.1016/j.renene.2019.05.124.
[37] Y. Jiang, M. Lawrence, M.P. Ansell, A. Hussain, Cell wall microstructure, pore size distribution and absolute density of hemp shiv, Royal Society Open Science. 5 (n.d.) 171945. https://doi.org/10.1098/rsos.171945.
[38] W. Zhang, X. Zhang, X. Zhang, Z. Yin, Y. Liu, M. Fang, X. Wu, X. Min, Z. Huang, Lauric-stearic acid eutectic mixture/carbonized biomass waste corn cob composite phase change materials: Preparation and thermal characterization, Thermochimica Acta. 674 (2019) 21–27. https://doi.org/10.1016/j.tca.2019.01.022.
[39] T. Dong, W. jiang, Y. liu, Y. Wu, Y. Qi, J. Li, Y. Ma, H. Ben, G. Han, A phase change material embedded composite consisting of kapok and hollow PET fibers for dynamic thermal comfort regulation, Industrial Crops and Products. 158 (2020) 112945. https://doi.org/10.1016/j.indcrop.2020.112945.
[40] A. Sarı, G. Hekimoğlu, V.V. Tyagi, Low cost and eco-friendly wood fiber-based composite phase change material: Development, characterization and lab-scale thermoregulation performance for thermal energy storage, Energy. 195 (2020) 116983. https://doi.org/10.1016/j.energy.2020.116983.
[41] G. Hekimoğlu, A. Sarı, T. Kar, S. Keleş, K. Kaygusuz, V.V. Tyagi, R.K. Sharma, A. Al-Ahmed, F.A. Al-Sulaiman, T.A. Saleh, Walnut shell derived bio-carbon/methyl palmitate as novel composite phase change material with enhanced thermal energy storage properties, Journal of Energy Storage. 35 (2021) 102288. https://doi.org/10.1016/j.est.2021.102288.
[42] I. Gómez-Arriaran, I. Sellens-Fernández, M. Odriozola-Maritorena, A. Erkoreka-González, A PC-tool to calculate the Moisture Buffer Value, Energy Procedia. 133 (2017) 68–75. https://doi.org/10.1016/j.egypro.2017.09.373.
[43] C. Rode, R. Peuhkuri, B. Time, K. Svennberg, T. Ojanen, Moisture Buffer Value of Building Materials, Heat-Air-Moisture Transport: Measurements on Building Materials. (2007). https://doi.org/10.1520/STP45403S.

[44] NF EN 12664, Afnor EDITIONS. (n.d.). https://www.boutique.afnor.org/fr-fr/norme/nf-en-12664/performance-thermique-des-materiaux-et-produits-pour-le-batiment-determinat/fa045168/18797 (accessed November 10, 2021).
[45] Norme NF EN 12667 Performance thermique des matériaux et produits pour le bâtiment. Détermination de la résistance thermique par la méthode de la plaque chaude gardée et la méthode fluxmétrique - Produits de haute et moyenne résistance thermique - AFNOR, n.d. https://www.decitre.fr/livres/norme-nf-en-12667-performance-thermique-des-materiaux-et-produits-pour-le-batiment-5552120005762.html (accessed November 10, 2021).
[46] E. Günther, S. Hiebler, H. Mehling, R. Redlich, Enthalpy of Phase Change Materials as a Function of Temperature: Required Accuracy and Suitable Measurement Methods, Int J Thermophys. 30 (2009) 1257–1269. https://doi.org/10.1007/s10765-009-0641-z.
[47] I. Petsagkourakis, E. Pavlopoulou, E. Cloutet, Y.F. Chen, X. Liu, M. Fahlman, M. Berggren, X. Crispin, S. Dilhaire, G. Fleury, G. Hadziioannou, Correlating the Seebeck coefficient of thermoelectric polymer thin films to their charge transport mechanism, Organic Electronics. 52 (2018) 335–341. https://doi.org/10.1016/j.orgel.2017.11.018.
[48] A.B. Kaiser, V. Skákalová, Electronic conduction in polymers, carbon nanotubes and graphene, Chem. Soc. Rev. 40 (2011) 3786–3801. https://doi.org/10.1039/C0CS00103A.
[49] O. Chung, S.-G. Jeong, S. Kim, Preparation of energy efficient paraffinic PCMs/expanded vermiculite and perlite composites for energy saving in buildings, Solar Energy Materials and Solar Cells. 137 (2015) 107–112. https://doi.org/10.1016/j.solmat.2014.11.001.
[50] C. Barreneche, J. Vecstaudza, D. Bajare, A.I. Fernandez, PCM/wood composite to store thermal energy in passive building envelopes, in: 2017. https://doi.org/10.1088/1757-899X/251/1/012111.
[51] X. Jingchen, Y. Keyan, Z. Yucheng, Y. Yuxiang, C. Jianmin, C. Liping, S.Q. Sheldon, Form-stable phase change material based on fatty acid/wood flour composite and PVC used for thermal energy storage, Energy and Buildings. 209 (2020) 109663. https://doi.org/10.1016/j.enbuild.2019.109663.
[52] T. Kar, A. Samanta, H. Sinnur, Studies on Effect of Application of Capric Acid and Stearic Acid based Reactive Phase Change Materials (rPCM) with PHAMS Binder on Thermal Comfort of Cotton Khadi Fabric as Thermo-tropic Smart Textiles., Journal of Natural Fibers. (2021) 1–20. https://doi.org/10.1080/15440478.2021.1880517.
[53] E. Terpakova, L. Kidalová, A. Estokova, J. Čigášová, N. Stevulova, Chemical Modification of Hemp Shives and their Characterization, Procedia Engineering. 42 (2012) 931–941. https://doi.org/10.1016/j.proeng.2012.07.486.
[54] P. Bouloc, S. Allegret, L. Arnaud, Hemp: industrial production and uses, CABI, Wallingford, 2013.
[55] L. Boussaba, G. Lefebvre, S. Makhlouf, A. Grados, L. Royon, Investigation and properties of a novel composite bio-PCM to reduce summer energy consumptions in buildings of hot and dry climates, Solar Energy. 214 (2021) 119–130. https://doi.org/10.1016/j.solener.2020.11.060.
[56] M. Dehmous, E. Franquet, N. Lamrous, Mechanical and thermal characterizations of various thermal energy storage concretes including low-cost bio-sourced PCM, Energy and Buildings. 241 (2021) 110878. https://doi.org/10.1016/j.enbuild.2021.110878.
[57] D.G. Atinafu, W. Dong, X. Huang, H. Gao, G. Wang, Introduction of organic-organic eutectic PCM in mesoporous N-doped carbons for enhanced thermal conductivity and energy storage capacity, Applied Energy. 211 (2018) 1203–1215. https://doi.org/10.1016/j.apenergy.2017.12.025.

[58] M. Asli, F. Brachelet, E. Sassine, E. Antczak, Thermal and hygroscopic study of hemp concrete in real ambient conditions, Journal of Building Engineering. 44 (2021) 102612. https://doi.org/10.1016/j.jobe.2021.102612.
[59] A. Sarı, A. Bicer, A. Karaipekli, F.A. Al-Sulaiman, Preparation, characterization and thermal regulation performance of cement based-composite phase change material, Solar Energy Materials and Solar Cells. 174 (2018) 523–529. https://doi.org/10.1016/j.solmat.2017.09.049.